Environmental Science & Technology

pubs.acs.org/est

Article

Modeling Clothing as a Vector for Transporting Airborne Particles and Pathogens across Indoor Microenvironments

Jacob Kvasnicka, Elaine A. Cohen Hubal, Jeffrey A. Siegel, James A. Scott, and Miriam L. Diamond*

Cite This: *Environ. Sci. Technol.* 2022, 56, 5641−5652

Read Online

ACCESS | Metrics & More | Article Recommendations | Supporting Information

ABSTRACT: Evidence suggests that human exposure to airborne particles and associated contaminants, including respiratory pathogens, can persist beyond a single microenvironment. By accumulating such contaminants from air, clothing may function as a transport vector and source of "secondary exposure". To investigate this function, a novel microenvironmental exposure modeling framework (ABICAM) was developed. This framework was applied to a para-occupational exposure scenario involving the deposition of viable SARS-CoV-2 in respiratory particles (0.5−20 μm) from a primary source onto clothing in a nonhealthcare setting and subsequent resuspension and secondary exposure in a car and home. Variability was assessed through Monte Carlo simulations. The total volume of infectious particles on the occupant's clothing immediately after work was 4800 μm^3 (5th−95th percentiles: 870−32 000 μm^3). This value was 61% (5−95%: 17−300%) of the occupant's primary inhalation exposure in the workplace while unmasked. By arrival at the occupant's home after a car commute, relatively rapid viral inactivation on cotton clothing had reduced the infectious volume on clothing by 80% (5−95%: 26−99%). Secondary inhalation exposure (after work) was low in the absence of close proximity and physical contact with contaminated clothing. In comparison, the average primary inhalation exposure in the workplace was higher by about 2−3 orders of magnitude. It remains theoretically possible that resuspension and physical contact with contaminated clothing can occasionally transmit SARS-CoV-2 between humans.

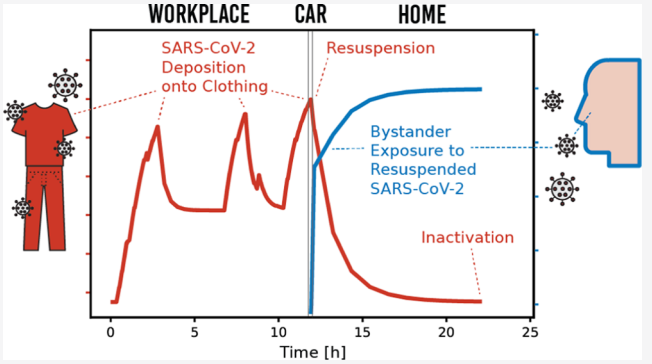

KEYWORDS: *SARS-CoV-2, virus, COVID-19, aerosol, droplet, para-occupational human exposure, particle resuspension, clothing, microenvironment, near-field exposure*

INTRODUCTION

Exposure to airborne particles and associated contaminants, including respiratory pathogens, is an important contributor to the global burden of disease.[1−3] Such exposure is especially important in indoor microenvironments where humans spend ~90% of their time on average.[4,5] While indoors, human occupants can considerably influence concentrations and dynamics of airborne particles. For instance, typical human activities can generate substantial concentrations of airborne particles indoors relative to background concentrations. Examples of such activities include cooking and other forms of surface heating, incomplete combustion (e.g., candles and incense),[6−9] vacuuming, and use of cleaning products,[10,11] ultrasonic essential oil diffusers,[12] and humidifiers.[13] In addition, nonsedentary activities (e.g., walking) can resuspend settled particles (dust).[14,15]

Occupants themselves can also release particles of both endogenous and exogenous origins. Once released, such particles can be directly inhaled or deposited onto surfaces such as clothing and/or skin whereby they can be resuspended and subsequently inhaled.[16−19] Examples of endogenous particles released by occupants include skin fragments[20] and respiratory particles, which may contain pathogens.[21] Examples of exogenous particles released by occupants include fragments of clothing fibers[20] and particles from external sources that have deposited onto the occupant's clothing and/or skin. These particles may include contaminants such as anemophilous pollen grains and fragments, bacteria, fungal spores, and particulate matter containing metals and sorbed semivolatile organic compounds.[22−26] Licina et al. have thoroughly reviewed the potential for clothing to function as a secondary source of such contaminants.[27]

Particle emissions from occupants and their activities, and corresponding exposures, can vary considerably both temporally and spatially. Regarding temporal variability, empirical

Received: December 8, 2021
Revised: March 19, 2022
Accepted: March 21, 2022
Published: April 11, 2022

https://doi.org/10.1021/acs.est.1c08342
Environ. Sci. Technol. 2022, 56, 5641−5652

evidence shows that typical human activities (e.g., cooking) can induce transient fluctuations in airborne particle concentrations.[8,9] These fluctuations can be investigated computationally using mass-balance models that are parameterized as functions of time-dependent human activities.[28]

Regarding spatial variability, convective airflows resulting from metabolic heat production, known as the "thermal plume", can efficiently transport particles released near an occupant into their breathing zone.[29,30] During periods of incomplete air mixing, such particles (and other contaminants) can accumulate into a "personal cloud". This cloud is an excess of concentration in an occupant's breathing zone relative to the room-average concentration.[15,31] The thermal plume and associated personal cloud typically exist only under conditions of relatively buoyant airflow with velocities generally less than 0.2 $m{\cdot}s^{-1}$.[32] As such, an occupant's thermal plume can be readily disrupted when they engage in nonsedentary activity.[15,30] Particles within the personal cloud of one occupant can also be transported into the breathing zones of other occupants (or "bystanders") in the same microenvironment. This phenomenon has been referred to as "cross-contamination".[15,33]

An additional, though less understood, factor that can influence particle exposure and variability is that occupants can visit multiple microenvironments (e.g., work, car, and home) throughout a typical day. Potential implications of visiting multiple microenvironments are twofold. First, an occupant may transport airborne particles across microenvironments and subsequently expose themselves and other occupants. This phenomenon has been hypothesized in the context of "para-occupational" exposure, whereby an individual "takes home" contaminants that had accumulated on their clothing and/or skin while in a workplace.[23,25,26,34] Second, visiting multiple microenvironments that contain a given contaminant would influence one's time-integrated or "cumulative" exposure to that contaminant. Accordingly, one's cumulative exposure would be a function of the time spent, activities, and other factors (e.g., ventilation) influencing contaminant dynamics within each microenvironment visited.

Cumulative exposure across microenvironments can be measured, given advances in particle sampling technology and statistical methods. Specifically, one can measure time-resolved particle concentrations in a person's breathing zone through personal sampling and apportion them to different recorded microenvironments and activities.[35,36] Such apportionment can provide accurate exposure estimates across microenvironments. However, it can be challenging to isolate and compare exposure pathways and other influential factors from measured data alone.

The purpose of this study was to develop a computational modeling framework to examine the joint influence of time-dependent human activities and indoor microenvironments on cumulative exposure to particles and associated contaminants. This framework leverages principles of mass balance, including fundamental processes of particle emission, transport, and fate, while accounting for temporal, spatial, and interindividual variabilities. In this study, the resulting framework was applied to an exposure scenario regarding severe acute respiratory syndrome coronavirus 2 (SARS-CoV-2), the virus responsible for the COVID-19 pandemic.

Abundant evidence suggests that the transmission of SARS-CoV-2 occurs predominantly indoors through inhaling relatively small, micron-scale respiratory particles.[2,3] Empirical evidence also suggests that clothing can mediate the transport and transmission of airborne viruses. For instance, clothing accumulated inhalable and respirable particles ($\leq$10 μm) from indoor air in experiments, which were then resuspended during typical human activities.[16−19] Such resuspension may have caused airborne SARS-CoV-2 genetic material (RNA) in protective-apparel removal rooms in a hospital environment.[37] Resuspension (or "aerosolized fomite") is also a suspected cause of the transmission of SARS-CoV-2 and influenza virus in controlled animal studies.[38−40] However, the potential for clothing to transmit SARS-CoV-2 between humans remains an open question.[41]

This study was motivated by the hypothesis that clothing can function as a transport vector for respiratory particles containing viable SARS-CoV-2 and, accordingly, a source of secondary exposure. The term "respiratory particles" is used herein to refer generally to aerosols or droplets that are expelled during human respiratory activities (e.g., breathing, speaking, etc.). This study focused on assessing the transport and fate of respiratory particles containing viable SARS-CoV-2 and associated inhalation exposure. Infection risk was not assessed because of associated uncertainties discussed in the Discussion section.

METHODS

Model Description and Components. This study further developed a computational modeling framework by Kvasnicka et al.[28] Herein, the algorithm is referred to as the Activity-Based Indoor Contaminant Assessment Model (ABICAM). ABICAM is a multicompartmental mass-balance modeling framework designed to simulate the dynamics of indoor contaminants and associated human exposure (for more information, visit https://abicam.org/). This study expanded the particle simulation module of ABICAM to be scalable across multiple indoor microenvironments and human occupants, facilitated by object-oriented programming. The resulting version of ABICAM had the following main components: indoor microenvironments, mass-balance models, human occupants, activities, activity schedules, data inputs, simulations, and exposure histories. Each of these components is described in the Supporting Information.

Model Formulation. In ABICAM, the dynamics of a given contaminant are represented by a system of coupled, first-order, ordinary, linear, inhomogeneous differential equations with time-dependent coefficients. Equation 1 represents this system of equations in a generalizable matrix notation. The Supporting Information includes a component-wise description of the specific mass balance developed and applied in this study (eqs S1−S7).

For a given mass-balance model associated with microenvironment e and contaminant c (which could be particles within a specific size range)

$$\frac{\mathrm{d}\overrightarrow{m_e^c}(t)}{\mathrm{d}t} = \boldsymbol{K}_e^c(\boldsymbol{t})\overrightarrow{m_e^c}(t) + \overrightarrow{E_e^c}(t) \quad (1)$$

where $\overrightarrow{m_e^c}(t)$ is a time-dependent vector of the mass of contaminant and $\boldsymbol{K}_e^c(\boldsymbol{t})$ is a square matrix (possibly sparse) of order n containing time-dependent mass transfer and removal rate coefficients $[T^{-1}]$, where n is the number of compartments. Diagonal elements of $\boldsymbol{K}_e^c(\boldsymbol{t})$ represent the sums of intercompartmental mass transfers and removals from the indoor system (e.g., through viral inactivation). Off-diagonal

https://doi.org/10.1021/acs.est.1c08342
Environ. Sci. Technol. 2022, 56, 5641−5652

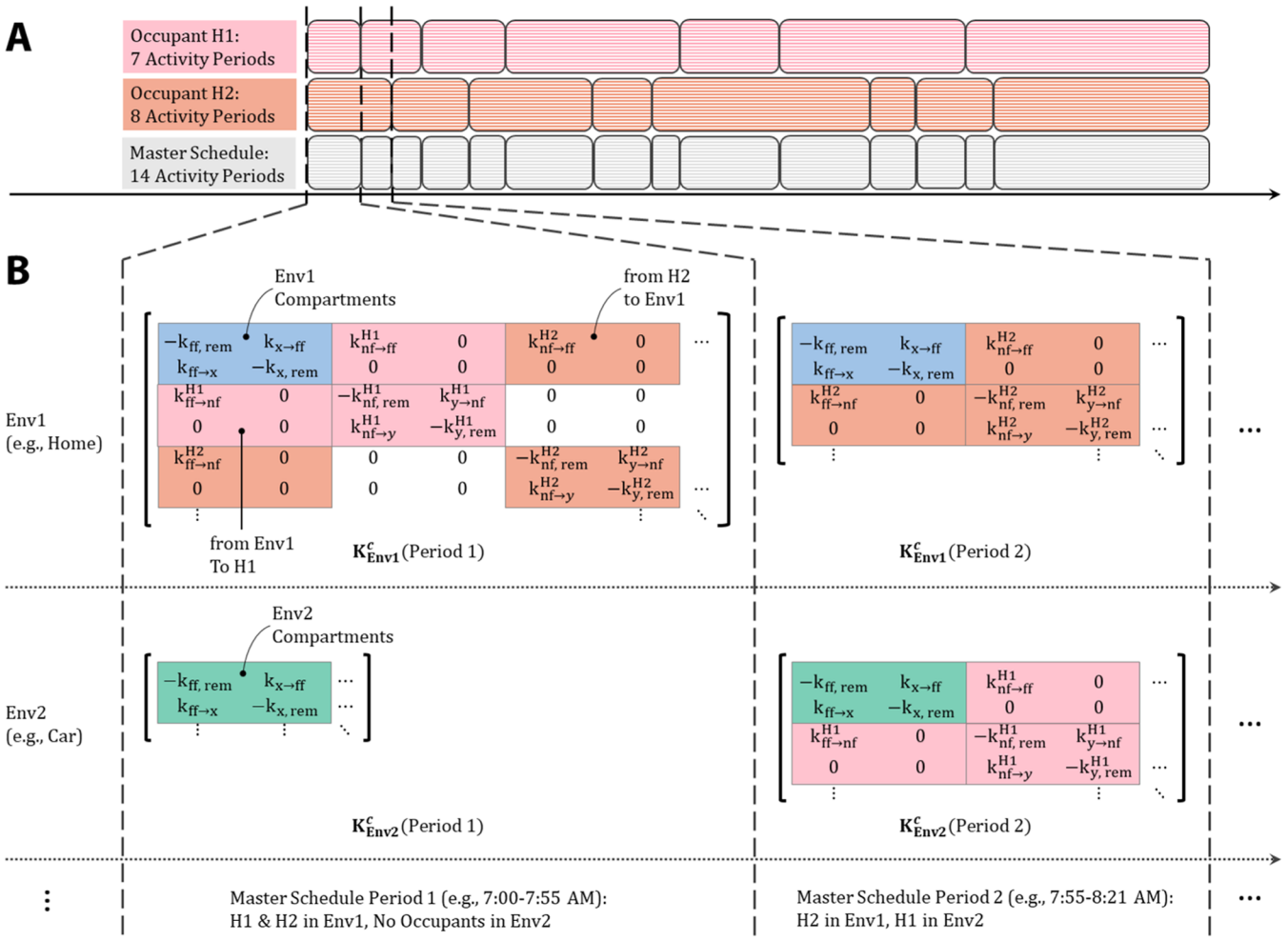

Figure 1. Overview of ABICAM's time-dependent matrices of rate coefficients for indoor microenvironments. (A) A "master schedule" maps the activities of two arbitrary human occupants (H1 and H2) to specific time periods. To illustrate, each activity period is represented by a superellipse with length directly proportional to duration. (B) For a given contaminant (c), each indoor microenvironment is associated with a matrix [$\boldsymbol{K}^{c}_{e}(t)$ in eq 1]. The size of each matrix reflects the total number of compartments in the microenvironment and therefore changes as human occupants enter and leave. In this example, H1 moves from Env1 to Env2 as time progresses from period 1 to period 2, while H2 remains in Env1. Rate coefficients [T^{-1}] for contaminant mass transfer (→) and removal (rem) are denoted by k with subscripts, nf, ff, x, and y referring to near-field, far-field, and arbitrary environmental and human compartments, respectively.

elements represent intercompartmental mass transfers (e.g., resuspension from clothing to air). $\overrightarrow{E^{c}_{e}}(t)$ is a vector of contaminant emission rates or source terms [$M{\cdot}T^{-1}$], which can also be time-dependent (e.g., exhalation of respiratory particles to air). The time dependences of $\boldsymbol{K}^{c}_{e}(t)$ and $\overrightarrow{E^{c}_{e}}(t)$ arise from the influence of human activities, as described by Kvasnicka et al.[28]

A near-field/far-field modeling approach was used to account for incomplete mixing between an occupant's thermal plume and the surrounding indoor air during static periods with relatively buoyant airflow.[42−45] If at least one occupant was present in a given microenvironment during a given time period, ABICAM discretized the indoor air compartment into a "far-field" plus one "near-field" for each occupant. The term "near-field" is used herein to refer to an occupant's thermal plume (see the Introduction section), while "far-field" corresponds to the surrounding indoor air. The concentration of a given contaminant in each air zone was assumed to be uniform ("well mixed").

The traditional near-field/far-field modeling approach[42−45] was modified to enable the disruption of the thermal plume during periods of rapid air mixing (e.g., by nonsedentary activity).[15] Exchanged airflows between zones were governed by a time-dependent (piecewise-constant) interzonal air exchange rate (AER). Accordingly, ABICAM could force a well-mixed condition in the indoor air compartment during any given period by applying a sufficiently high interzonal AER approximating the limit

$$\lim_{\substack{k^{h}_{nf\to ff}(t)\to\infty,\\ k^{h}_{ff\to nf}(t)\to\infty}} c^{h}_{nf}(t) = c_{ff}(t) \tag{2}$$

where $k^{h}_{nf\to ff}(t)$ and $k^{h}_{ff\to nf}(t)$ are rate coefficients in eq 1 [$\boldsymbol{K}^{c}_{e}(t)$], which were derived according to eqs S2 and S3 and represent contaminant mass transfer between the near-field (nf) of human occupant h and the far-field (ff); $c^{h}_{nf}(t)$ and $c_{ff}(t)$ are the corresponding contaminant concentrations [$M{\cdot}L^{-3}$] in each zone, respectively.

The near-field coupled a given human occupant and their compartments with the far-field compartment of the indoor

https://doi.org/10.1021/acs.est.1c08342
Environ. Sci. Technol. 2022, 56, 5641−5652

microenvironment in which they resided during a given period. If an occupant moved from one microenvironment to another, each respective microenvironment's network of compartments, and thus $K_e^c(t)$, was updated, as illustrated in Figure 1.

State Variable. The state variable chosen for this study was the equilibrium volume of respiratory particles containing viable SARS-CoV-2, net of viral inactivation. For brevity, we refer to such particles herein as "infectious particles". This volumetric state variable was chosen because of its potential to be used to estimate infection risk mechanistically (though such estimation of infection risk was left for future work). Previous modeling studies have performed such "bottom-up" estimations by (1) combining estimates of particle volume with empirical data on viral load to derive corresponding viral doses and then (2) combining these viral dose estimates with empirically derived dose−response relationships to estimate infection risks.[41,46−48] There are several uncertainties in estimating viral dose and corresponding infection risk based on particle volume, which are discussed in the Discussion section.

Scenario Description. The computational modeling framework described above was applied to a para-occupational exposure scenario regarding infectious particles. This scenario involved two human occupants and three indoor microenvironments across a 24 h period. The human occupants included two middle-aged adults (ages 30 to <41 years): one female and one male referred to herein as "HF" (human female) and "HM" (human male). Each occupant was represented by clothing and a general respiratory system. The model did not estimate internal doses of infectious particles to specific target tissues in the respiratory system because of uncertainties regarding how such doses relate to infection risk, as discussed in the Discussion section. Prior to the simulation, neither occupant had been exposed to SARS-CoV-2 (i.e., initial conditions were null).

The indoor microenvironments included a car, a workplace, and a home, which were also initially uncontaminated. Each microenvironment was represented by an indoor air compartment, which could be spatially discretized according to the near-field/far-field approach previously described (see the Model Formulation section). The home was modeled as a single-family detached residence in North America. For simplicity, the workplace was also modeled as such, though the parameter values for the home and workplace were chosen to be statistically independent. For the car, two different ventilation settings were separately examined: outside air intake and recirculation. Open-window configurations were not considered in this study but have been considered elsewhere.[49,50] For simplicity, the duration of time spent outdoors in transit between microenvironments (e.g., work to car) was chosen to be negligible. Consequently, the simulation did not include the potential for relatively rapid inactivation of SARS-CoV-2 by sunlight exposure, as observed in laboratory experiments.[51,52]

The simulation began with HF in the workplace where a single asymptomatic or presymptomatic index case emitted infectious particles into the far-field at a constant rate through breathing or speaking. HF did not come into close proximity to this index case, but she was exposed to these particles after complete mixing in the far-field. HM, in contrast, did not enter the workplace. After work, HF entered the car with HM, and the two occupants commuted to the home where they remained for the rest of the day. The occupants did not wear barrier face coverings during the simulation, which is a reasonable but "worst-case" assumption regarding inhalation exposure.

Model Parameterization. All input parameters were represented probabilistically with distributions statistically fit to empirical data from literature sources. Parameters pertaining to physical characteristics are used in eqs S1−S7, while those pertaining to human activities are used in eqs S8−S11. Tables S1−S4 summarize the corresponding probability distributions, which represent physical characteristics of the indoor microenvironments, human occupants, and respiratory particles, as well as human activities, respectively. For example, Table S2 summarizes the parameterization of the near-field volume and interzonal AER for a given occupant.

The clothing compartment of a given human occupant was parameterized according to a limited subset of common fabric types (Table S3). The inactivation rate coefficient of SARS-CoV-2 on clothing was based on empirical data limited to 100% cotton. It should be noted that this inactivation rate may be lower for some hydrophobic clothing materials (e.g., polyester), though empirical data were lacking.[53−55] The impact of a lower inactivation rate on the model's results was investigated in a separate sensitivity analysis described below.

For a given scenario, each parameter's probability density function was simulated using Monte Carlo sampling. Figure S1 shows convergence of the predicted secondary inhalation exposure percentiles with increasing sample size. The full simulation encompassed two car ventilation scenarios for a "base-case" simulation plus a sensitivity analysis described below. One Monte Carlo simulation (N = 10 000) required ∼9 h to run using parallel processing on a desktop computer with eight logical processors (Intel Core i7-2600 CPU @ 3.40 GHz, 3401 MHz).

Choice of Particle Equilibrium Size Range. Typical human respiratory activities can emit wide varieties of particles with diameters ranging from less than 1 μm to greater than 1000 μm.[21] Human inhalation exposure to SARS-CoV-2 generally concerns only a subset of these particles with diameters between about 0.1 μm and up to ∼100 μm.[41,56] Only those particles with diameters up to around 20 μm tend to remain airborne long enough to travel well beyond 1 m of the emission source under any airflow condition.[41] Accordingly, this study focused on respiratory particles with equilibrium diameters from 0.5 to 20 μm. Resuspension of smaller particles is likely negligible.[17] We inferred that all respiratory particles were predominantly solid, consisting of nonvolatile matter (or "droplet nuclei") that remained after near-instantaneous (<1 s) evaporation to equilibrium.[57]

Concentrations of respiratory particles can be well approximated by multimodal, log−normal functions of particle diameter.[21] In this study, however, a simpler approach was used to represent the size distribution. This approach facilitated ABICAM's parameterization and constrained its execution time and memory requirement. Specifically, particles with diameters <10 μm were discretized into three subranges based on their likely regions of penetration within the respiratory system: 0.5−2.5, 2.5−5, and 5−10 μm. Particles with diameters up to ∼10−15 μm tend to penetrate into the trachea and intrathoracic airways, while particles with diameters 2.5−5 μm deposit disproportionately in the respiratory bronchioles and alveoli.[58,59]

The remaining larger particles were grouped into a fourth size category (10−20 μm) for parameterization. In general, for

https://doi.org/10.1021/acs.est.1c08342
Environ. Sci. Technol. 2022, 56, 5641−5652

particles with diameters ≥10 μm, there was a lack of empirical data on deposition and resuspension rates for textiles such as clothing. As such, we extrapolated the values of these two parameters linearly from the smaller particle size range (5−10 μm) (Table S3). Consequently, results for the largest particle size range (10−20 μm) are more uncertain than for the three smaller size ranges.

Generation of Human Activity Schedules. This study focused on three general types of human "macroactivities": nonsedentary (e.g., walking), sedentary while awake (e.g., sitting), and sleeping. The specific activity that a given occupant was engaged in during a given period determined the values of their interzonal AER (eq 2 and Table S2), respiration rate (Table S2), and size-dependent resuspension rate coefficients (Table S3). Particle resuspension was assumed to conclude at the onset of sleeping, though the occupants could inhale any remaining resuspended particles while asleep.

Human activity schedules were generated probabilistically using empirical distributions from survey data (Table S4), combined with a set of rules to account for temporal dependencies between activities (see the Supporting Information, Generation of Human Activity Schedules section). Similar rules were developed and applied in previous simulations of human activities.[60,61]

Generating activity schedules occurred in two overarching stages. The first stage involved scheduling the time domains during which occupants resided in each indoor microenvironment. These time domains were chosen such that the occupants changed microenvironments simultaneously (e.g., car to home). The second stage involved scheduling individual activities within each microenvironment. The resulting schedules were tested to ensure accurate correspondence to the empirical survey data in Table S4.

Sensitivity Analysis. A sensitivity analysis was conducted with two objectives: (1) to identify the most influential model parameters with respect to the variability of several response variables for the base-case simulation described above and (2) to examine a plausible "worst-case" scenario assuming that viral inactivation did not occur during the simulated day.

For the first objective, Spearman rank correlation coefficients were computed to quantify monotonic relationships between the model's input parameters and response variables.[62] These coefficients measured the extent to which the parameters were both highly variable and propagated to a given model output. For parameters that are not strongly correlated with others, the squared coefficient can be used to approximate the percent contribution of a given input parameter to the variance of a given response variable (with respect to the ranked scores). Cumulative secondary inhalation exposures were chosen as the response variables for this analysis. For the second objective, the Monte Carlo simulation for each car ventilation scenario was rerun after setting the viral inactivation rate coefficient equal to zero. In other words, the volume of infectious particles equaled the equilibrium volume.

RESULTS

Exposure Assessment. For the base-case simulation, Figure 2 shows the time-average concentration of infectious particles in air, the corresponding net change in infectious particles on clothing, and the corresponding inhalation exposure of each human occupant for each indoor microenvironment. These distributions are log−normally distributed, and therefore, the median is used herein as the measure of central tendency. Figures S2 and S3 show examples of exposure histories from which these exposure distributions were derived. The remaining text differentiates between "primary exposure", which occurred in the workplace where the primary emission source (index case) was present, and "secondary exposure", which occurred after work because of resuspension of infectious particles from HF clothing.

Primary Exposure in the Workplace. HF spent an average of 9.8 h in the workplace [5th−95th percentiles (5−95%): 7.8−11.8 h] (Table S4). There, the index case emitted infectious particles at a constant rate into the far-field, resulting in a time-average concentration of 730 $\mu m^3 \cdot m^{-3}$ (5−95%: 190−2700 $\mu m^3 \cdot m^{-3}$) net of viral inactivation (Figure 2). The corresponding concentration in HF's near-field was lower by 9% (5−95%: 4−20%) due to the source-proximity effect and incomplete air mixing during periods of sedentary activity (eq 2).

By the end of the work period, HF had inhaled a total of 7800 μm^3 (5−95%: 1700−34 000 μm^3) of infectious particles (Figure 2). Relative contributions of each particle size range to this exposure were similar at 23% (0.5−2.5 μm), 21% (2.5−5 μm), 25% (5−10 μm), and 31% (10−20 μm) (Figure S4). In comparison, her clothing retained 4800 μm^3 (5−95%: 870−32 000 μm^3) of infectious particles (Figure 2). In other words, the total volume of infectious particles on her clothing available for secondary exposure after work was 61% (5−95%: 17−300%) of her primary inhalation exposure in the workplace. Most (87%) of this total volume on clothing originated from particles with equilibrium diameters greater than 5 μm (Figure S4).

Secondary Exposures in the Car. After work, HF entered the car with HM, and the two occupants commuted home together for an average duration of 21 min (5−95%: 10−47 min) (Table S4). During this period, concentrations of infectious particles and associated exposures depended on which car ventilation setting was used.

Under recirculation, the time-average concentration of infectious particles in the well-mixed car cabin air was 7.0 $\mu m^3 \cdot m^{-3}$ (5−95%: 0.92−75 $\mu m^3 \cdot m^{-3}$) due to low-intensity resuspension from HF's clothing while seated. Compared to the workplace, this concentration was lower by a factor of 110 (5−95%: factor of 13−560). HF's inhalation exposure was also lower in the car by a factor of 2700 (5−95%: factor of 290−12 000) because of the reduced airborne concentrations and exposure duration compared to the workplace. HM's inhalation exposure in the car was higher than that of HF by 35%, on average, because he tended to have a higher respiration rate (Table S2).

Under the alternative ventilation scenario of the outside air intake, the median AER in the car cabin increased by a factor of 11 (5−95%: factor of 5−24) relative to recirculation (Table S1). Accordingly, the inhalation exposures of the occupants were reduced by 58% (5−95%: 46−72%) (Figure 2). During the car commute, the total volume of infectious particles on HF's clothing decreased by 80% (5−95%: 26−99%) (Figure 2). This decrease was driven by the relatively high inactivation rate of SARS-CoV-2 on 100% cotton clothing compared to that of air (Table S3).

Secondary Exposures in the Home. After the commute, the occupants entered the home where they remained awake for an additional 5.5 h (5−95%: 2.3−8.6 h) (as derived from eqs S8−S11 with parameterization listed in Table S4). There, the time-average concentration of infectious particles in HF's near-field

https://doi.org/10.1021/acs.est.1c08342
Environ. Sci. Technol. 2022, 56, 5641−5652

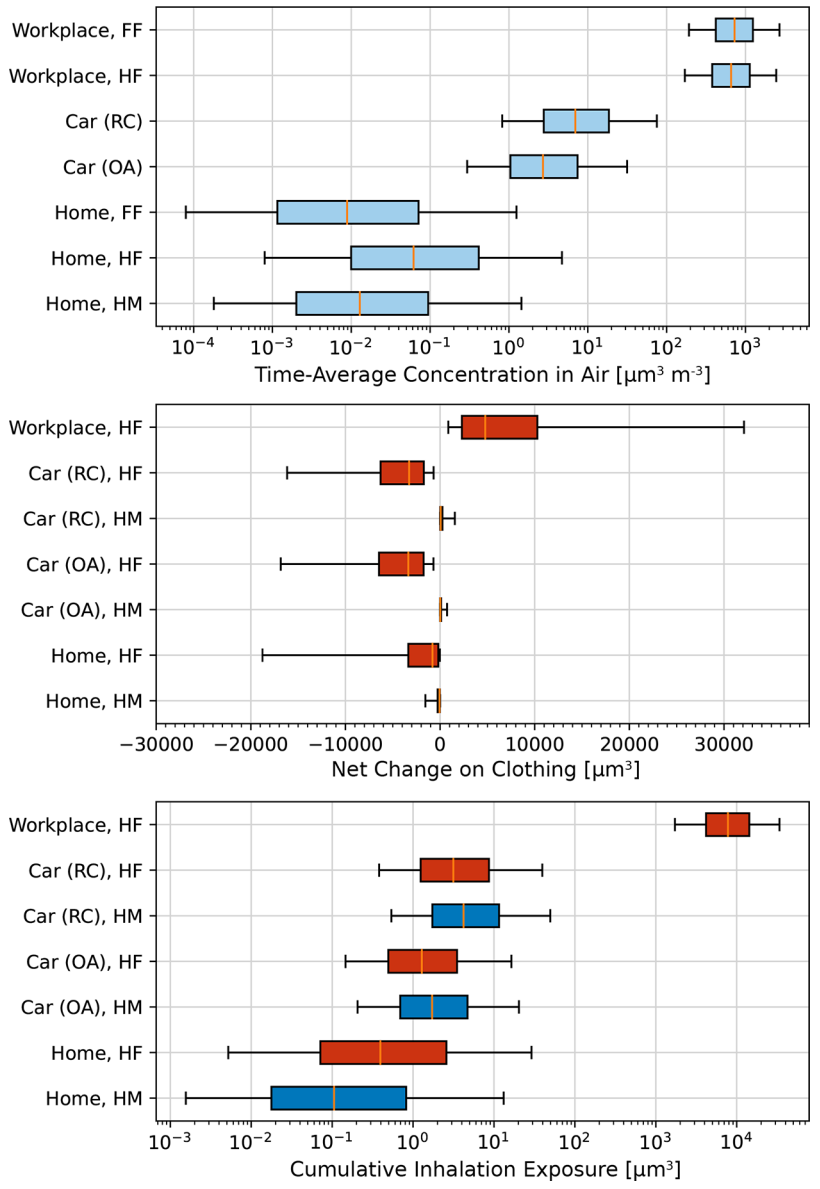

Figure 2. Time-average concentrations of infectious particles and corresponding exposures for each indoor microenvironment and human occupant. For a given microenvironment, airborne concentrations correspond to either the far-field (FF) or near-field of a given human occupant (HF or HM). "OA" and "RC" refer to the car ventilation scenarios of outside air intake (windows closed) and recirculation, respectively. For the home, results are shown for the RC scenario (differences in medians between scenarios were <10%). Boxes extend from the first to third quartile values of predictions, with a line at the median. Whiskers are truncated at the 5th and 95th percentiles.

was lower than that of the car cabin by factors of 530 and 290 for the car ventilation scenarios of recirculation and outside air intake, respectively (Figure 2). In the home, the time-average concentration in HF's near-field was higher than that of the far-field by a factor of 5 (95%: factor of 1−26). This near-field concentration enhancement was due to the source-proximity effect under incomplete air mixing (i.e., higher concentration near HF because her clothing was the source). Nonetheless, inhalation exposures to infectious particles at home were minimal, with at most 0.39 μm^3 (95%: 29 μm^3) being inhaled by HF under the car ventilation scenario of recirculation. By the end of the day, 100% of infectious virions on HF's clothing had been inactivated (5th through 95th percentiles).

Cumulative Exposures across Indoor Microenvironments. Figure 3 shows the range of distributions of cumulative secondary inhalation exposure to infectious particles from resuspension across indoor microenvironments. Two additional distributions are shown for comparison: (1) the corresponding volume of infectious particles on HF's clothing available for secondary exposure after work and (2) her primary inhalation exposure in the workplace. The former represents the maximum theoretically possible secondary exposure that could occur. The predicted average secondary inhalation exposures ranged up to 4.4 μm^3 (5−95%: 0.55−64 μm^3) for HM under the car ventilation scenario of recirculation, while HF's primary inhalation exposure in the workplace was higher by an average factor of 1800 (5−95%: factor of 160−9500).

Figure S5 compares the percent contributions of each indoor microenvironment to the occupants' cumulative inhalation exposures across the 24 h simulation. Practically, 100% of HF's cumulative exposure occurred in the workplace where the

https://doi.org/10.1021/acs.est.1c08342
Environ. Sci. Technol. 2022, 56, 5641−5652

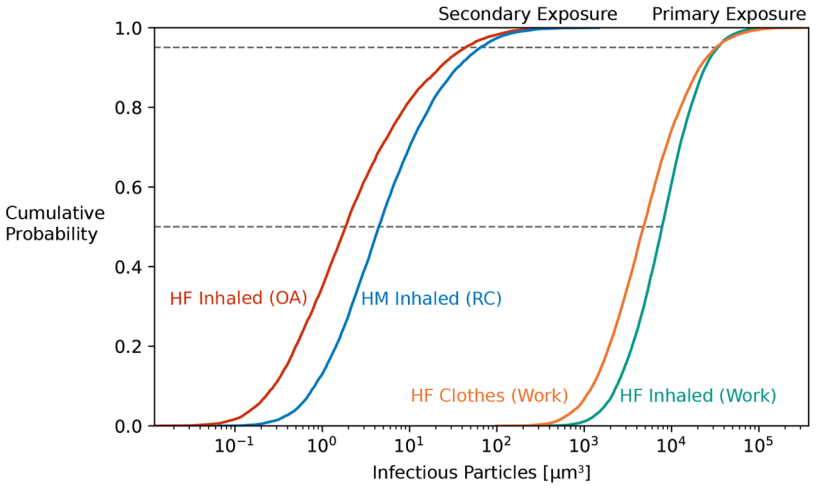

Figure 3. Distributions of primary versus secondary exposure to infectious particles. Secondary exposure distributions represent cumulative inhalation exposures to resuspended particles, deposited from the primary source, across the car and home microenvironments. The distribution of infectious particles on clothing is the final condition while in the workplace and represents infectious particles available for secondary exposure. "HF" and "HM" refer to the human female and male adult occupants, respectively. "OA" and "RC" refer to the car ventilation scenarios of outside air intake (windows closed) and recirculation, respectively. Horizontal lines indicate the 50th and 95th percentiles.

primary emission source was present. In contrast, 96−98% of HM's average cumulative exposure occurred in the car due to cross-contamination by HF's clothing under the car ventilation scenarios of outside air intake and recirculation, respectively. Most (>90%) of the occupants' cumulative secondary inhalation exposures originated from particles with equilibrium diameters greater than 5 μm (Figure S4).

Sensitivity Analysis. *Parameter Contributions to Prediction Variability.* For the base-case simulation, Figure S6 shows the Spearman rank correlation coefficients (ρ) between the model's input parameters and response variables (cumulative secondary inhalation exposures). These coefficients are rank-ordered by their contributions to the variance of each response variable, as approximated by ρ^2. In all cases, the viral inactivation rate coefficient for 100% cotton clothing had the greatest influence, contributing ∼48−61% of the variances (i.e., ρ^2: 0.48−0.61). For particles ≤5 μm, the primary emission rate of infectious particles in the workplace and the volume of the workplace ranked second and third, respectively, with similar variance contributions (ρ^2: 0.090−0.14). For larger particles, the primary emission rate was less important regarding its variance contribution ($\rho^2 \leq 0.086$), while the volume of the workplace consistently ranked second (ρ^2: 0.13−0.17).

For the remaining parameters, the rank order depended on the occupant and car ventilation scenario, in addition to particle size. These influential parameters included particle characteristics [e.g., deposition rate coefficient for indoor surfaces (ρ^2: 0.026−0.11)], physical human characteristics [e.g., respiration rate (ρ^2: 0.021−0.071)], and building characteristics [e.g., AER of the workplace (ρ^2: 0.016−0.022)]. Particle deposition in the car was not included in this analysis because of a lack of measured deposition rate coefficients for the particle size range considered in this study.

Assumption of Null Inactivation Rates. Considering that the viral inactivation rate coefficient for clothing was the most influential parameter in the base-case simulation (Figure S6), Figures S7 and S8 compare ABICAM's predictions under the "worst-case" assumption that viral inactivation did not occur. Relative to the base-case simulation (Figure 2), cumulative secondary inhalation exposures increased under this assumption but were still lower than HF's primary inhalation exposure in the workplace by at least a factor of 85 (5−95%: factor of 34−220). The workplace contributed 99% of HF's average cumulative inhalation exposure (Figure S5). The total volume of infectious particles on her clothing available for secondary exposure after work increased to 3 times (5−95%: 1−9 times) her primary inhalation exposure in the workplace.

Regarding secondary exposure, the importance of the car versus the home depended on the car ventilation scenario (Figure S5). Under recirculation, 61% of HM's average cumulative inhalation exposure occurred in the car. In contrast, 59% of this exposure occurred at home under the scenario of outside air intake. These findings contrasted with those of the base-case simulation in which secondary exposure occurred predominantly in the car. Again, most (66−75%) of the occupants' cumulative secondary inhalation exposures originated from particles with equilibrium diameters greater than 5 μm (Figure S4).

DISCUSSION

In this study, a novel computational modeling framework (ABICAM) was expanded to examine the joint influence of time-dependent human activities and indoor microenvironments on cumulative exposure to respiratory particles containing viable SARS-CoV-2. Resuspension of pathogens from clothing and other surfaces has been an open question, and to the best of our knowledge, there are no previous estimates of SARS-CoV-2 resuspension from clothing and associated exposure. Moreover, the treatment of the interzonal airflow rate as a dynamic parameter accounting for factors such as human movement (eq 2) provided an enhancement to typical approaches.[42−45] ABICAM is also generalizable to other exposure scenarios and contaminants, including those in the gas phase (e.g., semivolatile organic compounds).

Overall, the results support the hypothesis that clothing can function as a transport vector for respiratory particles containing viable SARS-CoV-2 and, accordingly, a source of secondary exposure. However, the magnitudes of predicted secondary inhalation exposures to infectious particles (0.5−20

https://doi.org/10.1021/acs.est.1c08342
Environ. Sci. Technol. 2022, 56, 5641−5652

μm) resuspended from clothing were minimal compared to those of primary inhalation exposure in the workplace. The relatively high inactivation rates of SARS-CoV-2 observed on porous 100% cotton,[53,54] in conjunction with the empirically based rates of particle deposition onto clothing and subsequent resuspension (Table S3), resulted in secondary inhalation exposures that were lower than the primary inhalation exposure by 3 orders of magnitude on average (Figure 3). Even under conditions that promoted SARS-CoV-2 viability (e.g., wearing hydrophobic clothing materials),[53,55] secondary inhalation exposures were still lower than the primary inhalation exposure by about 2 orders of magnitude on average (Figure S8).

As with any simulation-based study, ours had limitations. First, a lack of empirical data precluded model evaluation. In general, modeling clothing as a vector for transporting and resuspending airborne particles and pathogens is difficult because of uncertainties in many of the associated parameters. Monte Carlo simulations and sensitivity analyses were conducted to assess the implications of these parameter uncertainties on the model's predictions. However, there may be unquantified biases in the absolute results due to the model's formulation and/or simplifying assumptions made. In contrast, relative results (e.g., percent change in exposure estimates between different microenvironments or scenarios) convey only quantitative trends but can reduce the perception of certainty and be more stable to such biases.

An additional limitation of this study stemmed from the lack of any assessment of infection risk, which limits the ability to interpret the results from a public health perspective. As noted, the volume of infectious particles was chosen as the exposure metric based on its potential to be used to estimate infection risk mechanistically (see the State Variable section). However, several uncertainties in estimating viral dose and corresponding infection risk based on particle volume are worth noting. First, viral loads of infected humans can vary by several orders of magnitude depending on the individual and the timing of sample collection relative to the disease course.[41] In addition, SARS-CoV-2 is likely to be inhaled as a mixture of ultrafine virions and virion clusters. The concentration of virions in respiratory emissions therefore probably depends on particle size,[63−65] which, in turn, depends on the site of origin in the respiratory system and associated particle formation mechanisms.[41] Consequently, the number of SARS-CoV-2 virions in respiratory emissions, and therefore infectivity, probably does not scale directly with total particle volume but instead with the volume of exhaled particles within specific size ranges. Accordingly, we have reported the percent contributions of each particle size range (Figure S4) to supplement the exposure estimates (Figures 2, 3, S7, and S8).

Furthermore, it is difficult to accurately measure the infectivity of respiratory particles across a sufficiently broad particle size range because the collection and analytical methods themselves interfere with the viability of sampled virions.[64,66] In the absence of such data, other modeling studies have used RNA copies as a surrogate for infectivity.[48,67] However, RNA does not necessarily indicate the presence of infectious virions. For instance, measured SARS-CoV-2 RNA persisted for days on a variety of surfaces, including porous 100% cotton, despite significant reductions in viability as measured by the median tissue culture infectious dose ($TCID_{50}$).[53] Lastly, the dose−response relationship for SARS-CoV-2 will likely vary with vaccination status and viral variant and is not necessarily linear nor consistent across particle sizes and exposure routes.[47,68]

An additional limitation of our study was the model's relatively simplified representation of particle mass-transfer mechanisms. A more accurate representation could be accomplished with a physics-based computational fluid dynamics model, especially for scenarios involving close proximity between occupants (<1.4−1.6 m).[33,48] However, the substantial data and computational requirements of such models generally limit their applicability to deterministic scenarios involving a single, well-characterized environment with minimal human influence. In comparison, the approach used in this study was consistent with the limited data available for parameterization and facilitated a probabilistic characterization of variability requiring tens of thousands of executions of the algorithm.

As noted, the simulations did not include particle deposition losses in the car due to a lack of measured data required for parameterization. These losses may be appreciable due to relatively high air velocities and surface-area-to-volume ratios in cars compared to other indoor microenvironments (e.g., residences).[69] Including these losses in the simulations would have reduced the magnitudes of secondary inhalation exposure, which, in turn, would have increased the relative importance of the primary exposure event.

This study was also constrained to a specific exposure scenario and associated human activities. The exposure scenario was developed to be relevant to the general population, in accordance with the availability of data for model parameterization. It remains possible that other scenarios and associated activities correspond to greater risks of clothing-mediated exposure to SARS-CoV-2. For instance, healthcare workers may encounter several COVID-19 cases throughout a given work shift and perform high-risk activities such as aerosol-generating medical procedures.[70] One specific concern for healthcare workers is the potential for viral-laden particles to be resuspended by doffing personal protective equipment (e.g., after a work shift),[37] which could be investigated. However, it is unclear whether healthcare workers are at a greater risk of exposure compared to this study given the frequent use of precautionary measures in healthcare settings (e.g., enhanced ventilation, personal protective equipment, surface cleaning, etc.).[70]

The exposure scenario in this study did not include the use of personal protective equipment, such as barrier face coverings. As noted, excluding such coverings is a reasonable but "worst-case" assumption regarding inhalation exposure. Wearing such coverings in the workplace could have reduced the magnitude of primary inhalation exposure which, in turn, would have increased the relative importance of secondary inhalation exposures. However, it is likely that these secondary inhalation exposures would still be relatively low. For these exposures to be of similar magnitudes as primary exposure, barrier face coverings would have had to filter $\geq$ 99% of the total volume of infectious particles that would have otherwise been inhaled by HF in the workplace. This high level of filtration might only be achieved by a well-fitted respirator mask.[41]

The exposure scenario was also limited to a few general "macroactivities", which were parameterized according to empirical survey data (Table S4).[60] Empirical data on activity parameters and particle resuspension rate coefficients were unavailable for plausible shorter duration activities that might

https://doi.org/10.1021/acs.est.1c08342
Environ. Sci. Technol. 2022, 56, 5641−5652

also resuspend particles from clothing. Such "microactivities" may include hugging, donning or doffing clothing, and removing a backpack or shoulder bag. In addition, handling friable textile materials, such as homemade cotton facemasks, has been shown to release nonexpiratory micron-scale particles,[71] which could be subsequently inhaled. ABICAM could account for such microactivities if corresponding data become available.

This study also did not include the potential for exposure at close proximity in the workplace because of associated uncertainties regarding human microactivities and particle transport. This assumption is reasonable, especially if physical distancing is maintained as a precautionary measure. However, at close proximity, a bystander would likely be exposed to a higher concentration of respiratory particles, especially larger, predominantly liquid particles.[41,48,72,73] Such larger, predominately liquid particles may not have had sufficient time to fully evaporate to solid droplet nuclei prior to depositing onto an occupant's clothing.[41]

The potential for larger, predominantly liquid particles on clothing to cause infection is uncertain because of several factors. First, empirical evidence suggests that such particles emitted by humans with COVID-19 have lower concentrations of SARS-CoV-2 compared to smaller particles (e.g., $\leq$5 μm) that originate from the lower respiratory system.[63−65] This concentration enrichment of virions in smaller particles has also been observed for other respiratory pathogens, such as influenza virus.[74] However, as noted, particles of different sizes tend to deposit in different regions within the respiratory system,[58,59] and it is unclear whether this deposition in different regions influences COVID-19 infection risk and severity.

In addition to particle size, the type of clothing material onto which larger liquid particles deposit may also influence their infectivity. For instance, hydrophilic textile fibers (e.g., 100% cotton) can readily absorb liquid particles through capillary action, leaving the virus's lipid membrane susceptible to desiccation.[75] These mechanisms may have caused the relatively rapid inactivation of SARS-CoV-2 and similar coronaviruses observed on porous 100% cotton fabric in laboratory experiments.[53−55] It should be noted that measured inactivation rates of SARS-CoV-2 on textiles, such as clothing, were scarce [and hence the choice of a uniform distribution in this study (Table S3)]. The available measurements were also highly variable, with values spanning 2 orders of magnitude between studies. Consequently, the inactivation rate of SARS-CoV-2 on clothing was the most influential parameter in this study (Figure S6). The large variability of this parameter may relate to interstudy differences (e.g., in the material attributes of the textiles used and/or virus preparation).[53,54]

In addition to inactivation, the type of clothing material may also influence the resuspension of larger liquid particles in a manner that differs from solid particles. Experiments have indicated that the mass fraction of solid particles deposited onto clothing that subsequently resuspend depends on particle size, the type of clothing material or weave pattern, and the type of removal force applied, which depends on the activity.[16−19] However, as noted, available measurements of particle resuspension from clothing have been limited to solid particles with diameters $\leq$10 μm. Results from previous modeling suggest that liquid particles can undergo fragmentation prior to resuspension, depending on the material's hydrophobicity, as well as particle size and removal force.[76,77] Such fragmentation may have consequences for particle exposure and infectivity.

Besides resuspension, physical contact with clothing as a fomite is a plausible exposure pathway, especially for the wearer of the clothing. Such contact may contribute to infection risk through either of the following pathways: (1) direct transfer of virions from clothing to mucosa on the face (nose, mouth, or eyes) and (2) indirect transfer of virions from clothing to such mucosa mediated by hands. Exposure to SARS-CoV-2 from physical contact with clothing would depend on the frequency and nature of contact (e.g., surface area contacted and pressure exerted), in addition to the type of clothing material and physical characteristics of the contaminant.[78,79] Measured data were lacking on the transfer of enveloped viruses such as SARS-CoV-2 between clothing and skin. However, measured data for nonporous surfaces suggest that greater surface roughness results in less efficient transfer compared to smooth surfaces.[79]

While physical contact with clothing as a fomite may contribute to infection risk, a higher applied dose may be required to elicit the same physiological response as inhalation. In an animal study involving Syrian hamsters, for instance, airborne transmission of SARS-CoV-2 was more efficient and resulted in higher viral loads and more severe disease manifestations than fomite transmission.[68] If these findings are applicable to humans, COVID-19 is "anisotropic", meaning that the dose−response relationship and/or virulence of infection depends on the target tissue and, accordingly, the exposure route.[80]

Lastly, other plausible activities outside the scope of this study could effectively decontaminate clothing containing SARS-CoV-2 or other pathogens, thereby reducing the likelihood of secondary exposure. Such activities include exposure of clothing to ultraviolet radiation, as can occur by sunlight outdoors, and domestic laundering. In laboratory experiments, simulated sunlight increased the inactivation rate of SARS-CoV-2 in aerosols and on stainless steel surfaces by ~1 order of magnitude relative to conditions resembling indoors or nighttime.[51,52] In a different experiment, domestic clothes washing at ambient temperature (23° C) with detergent reduced the infectious viral titer of a model human coronavirus (HCoV-OC43) on 100% cotton textiles below the assay's detection limit (1.5 $\log_{10}$ $TCID_{50}$ 25 cm^{-2} material).[55] One should limit physically disturbing clothing prior to laundering them, however, to minimize particle resuspension.

In sum, the findings of this study suggest that secondary inhalation exposure to viable SARS-CoV-2 resuspended from clothing is typically low compared to primary inhalation exposure in a nonhealthcare setting. It remains theoretically possible that resuspension and physical contact with clothing as a fomite can occasionally transmit SARS-CoV-2 between humans. The computational modeling framework developed in this study can serve as a heuristic tool for synthesizing the disparate information required to understand the relative importance of exposure pathways for pathogens and other contaminants indoors.

■ ASSOCIATED CONTENT

Supporting Information

The Supporting Information is available free of charge at https://pubs.acs.org/doi/10.1021/acs.est.1c08342.

https://doi.org/10.1021/acs.est.1c08342
Environ. Sci. Technol. 2022, 56, 5641−5652

Component-wise description of the mass balance of infectious particles (eqs S1−S7), description of the probabilistic approach used to generate human activity schedules (eqs S8−S11), summaries of model parameterization (Tables S1−S4), and supplemental results including those from the sensitivity analysis (Figures S1−S8) (PDF)

AUTHOR INFORMATION

Corresponding Author

Miriam L. Diamond − *Department of Earth Sciences, University of Toronto, Toronto, Ontario M5S 3B1, Canada; School of the Environment, University of Toronto, Toronto, Ontario M5S 3E8, Canada; Dalla Lana School of Public Health, University of Toronto, Toronto, Ontario M5T 3M7, Canada;* orcid.org/0000-0001-6296-6431; Phone: 1 (416) 978-1586; Email: miriam.diamond@utoronto.ca

Authors

Jacob Kvasnicka − *Department of Earth Sciences, University of Toronto, Toronto, Ontario M5S 3B1, Canada;* orcid.org/0000-0002-8076-9703

Elaine A. Cohen Hubal − *Center for Public Health and Environmental Assessment, U.S. Environmental Protection Agency, Durham, North Carolina 27711, United States;* orcid.org/0000-0002-9650-3483

Jeffrey A. Siegel − *Department of Civil and Mineral Engineering, University of Toronto, Toronto, Ontario M5S 1A4, Canada; Dalla Lana School of Public Health, University of Toronto, Toronto, Ontario M5T 3M7, Canada;* orcid.org/0000-0001-5904-169X

James A. Scott − *Dalla Lana School of Public Health, University of Toronto, Toronto, Ontario M5T 3M7, Canada; Department of Laboratory Medicine and Pathobiology, Temerty Faculty of Medicine, University of Toronto, Toronto, Ontario M5S 1A8, Canada*

Complete contact information is available at: https://pubs.acs.org/10.1021/acs.est.1c08342

Notes

The views expressed in this article are those of the authors and do not necessarily represent the views or policies of the U.S. Environmental Protection Agency.

The authors declare no competing financial interest.

ACKNOWLEDGMENTS

The authors thank John Ladan (University of Toronto) for constructive feedback on the algorithm design, Emma McLay (University of Toronto) for her assistance with data collection, and Drs. Katherine Ratliff, Tim Wade, and Shawn Ryan (U.S. EPA) for their feedback on an earlier draft of this manuscript. Funding was provided by the Natural Sciences and Engineering Research Council (NSERC) RGPIN-2017-06654 to M.L.D. and the University of Toronto to support J.K.

REFERENCES

(1) Cohen, A. J.; Brauer, M.; Burnett, R.; Anderson, H. R.; Frostad, J.; Estep, K.; Balakrishnan, K.; Brunekreef, B.; Dandona, L.; Dandona, R.; et al. Estimates and 25-Year Trends of the Global Burden of Disease Attributable to Ambient Air Pollution: An Analysis of Data from the Global Burden of Diseases Study 2015. *Lancet* **2017**, *389*, 1907−1918.

(2) Greenhalgh, T.; Jimenez, J. L.; Prather, K. A.; Tufekci, Z.; Fisman, D.; Schooley, R. Ten Scientific Reasons in Support of Airborne Transmission of SARS-CoV-2. *Lancet* **2021**, *397*, 1603−1605.

(3) Tang, J. W.; Marr, L. C.; Li, Y.; Dancer, S. J. Covid-19 Has Redefined Airborne Transmission. *Br. Med. J.* **2021**, *373*, No. n913.

(4) Klepeis, N. E.; Nelson, W. C.; Ott, W. R.; Robinson, J. P.; Tsang, A. M.; Switzer, P.; Behar, J. V.; Hern, S. C.; Engelmann, W. H. The National Human Activity Pattern Survey (NHAPS): A Resource for Assessing Exposure to Environmental Pollutants. *J. Exposure Sci. Environ. Epidemiol.* **2001**, *11*, 231.

(5) Leech, J. A.; Nelson, W. C.; T Burnett, R.; Aaron, S.; Raizenne, M. E. It's about Time: A Comparison of Canadian and American Time−Activity Patterns. *J. Exposure Sci. Environ. Epidemiol.* **2002**, *12*, 427.

(6) Wallace, L. Indoor Sources of Ultrafine and Accumulation Mode Particles: Size Distributions, Size-Resolved Concentrations, and Source Strengths. *Aerosol Sci. Technol.* **2006**, *40*, 348−360.

(7) Wallace, L. A.; Ott, W. R.; Weschler, C. J.; Lai, A. C. Desorption of SVOCs from Heated Surfaces in the Form of Ultrafine Particles. *Environ. Sci. Technol.* **2017**, *51*, 1140−1146.

(8) Patel, S.; Sankhyan, S.; Boedicker, E. K.; DeCarlo, P. F.; Farmer, D. K.; Goldstein, A. H.; Katz, E. F.; Nazaroff, W. W.; Tian, Y.; Vanhanen, J.; et al. Indoor Particulate Matter during HOMEChem: Concentrations, Size Distributions, and Exposures. *Environ. Sci. Technol.* **2020**, *54*, 7107−7116.

(9) Tian, Y.; Arata, C.; Boedicker, E.; Lunderberg, D. M.; Patel, S.; Sankhyan, S.; Kristensen, K.; Misztal, P. K.; Farmer, D. K.; Vance, M.; et al. Indoor Emissions of Total and Fluorescent Supermicron Particles during HOMEChem. *Indoor Air* **2021**, *31*, 88−98.

(10) Corsi, R. L.; Siegel, J. A.; Chiang, C. Particle Resuspension during the Use of Vacuum Cleaners on Residential Carpet. *J. Occup. Environ. Hyg.* **2008**, *5*, 232−238.

(11) Singer, B. C.; Coleman, B. K.; Destaillats, H.; Hodgson, A. T.; Lunden, M. M.; Weschler, C. J.; Nazaroff, W. W. Indoor Secondary Pollutants from Cleaning Product and Air Freshener Use in the Presence of Ozone. *Atmos. Environ.* **2006**, *40*, 6696−6710.

(12) Schwartz-Narbonne, H.; Du, B.; Siegel, J. A. Volatile Organic Compound and Particulate Matter Emissions from an Ultrasonic Essential Oil Diffuser. *Indoor Air* **2021**, *31*, 1982−1992.

(13) Lau, C. J.; Loebel Roson, M.; Klimchuk, K. M.; Gautam, T.; Zhao, B.; Zhao, R. Particulate Matter Emitted from Ultrasonic Humidifiers—Chemical Composition and Implication to Indoor Air. *Indoor Air* **2021**, *31*, 769−782.

(14) Ferro, A. R.; Kopperud, R. J.; Hildemann, L. M. Elevated Personal Exposure to Particulate Matter from Human Activities in a Residence. *J. Exposure Sci. Environ. Epidemiol.* **2004**, *14*, S34−S40.

(15) Licina, D.; Tian, Y.; Nazaroff, W. W. Emission Rates and the Personal Cloud Effect Associated with Particle Release from the Perihuman Environment. *Indoor Air* **2017**, *27*, 791−802.

(16) Ren, J.; Tang, M.; Novoselac, A. Experimental Study to Quantify Airborne Particle Deposition onto and Resuspension from Clothing Using a Fluorescent-Tracking Method. *Build. Environ.* **2021**, *209*, No. 108580.

(17) Licina, D.; Nazaroff, W. W. Clothing as a Transport Vector for Airborne Particles: Chamber Study. *Indoor Air* **2018**, *28*, 404−414.

(18) McDonagh, A.; Byrne, M. A. The Influence of Human Physical Activity and Contaminated Clothing Type on Particle Resuspension. *J. Environ. Radioact.* **2014**, *127*, 119−126.

(19) McDonagh, A.; Byrne, M. A. A Study of the Size Distribution of Aerosol Particles Resuspended from Clothing Surfaces. *J. Aerosol Sci.* **2014**, *75*, 94−103.

(20) Yang, S.; Bekö, G.; Wargocki, P.; Williams, J.; Licina, D. Human Emissions of Size-Resolved Fluorescent Aerosol Particles: Influence of Personal and Environmental Factors. *Environ. Sci. Technol.* **2021**, *55*, 509−518.

(21) Pöhlker, M. L.; Krüger, O. O.; Förster, J.-D.; Berkemeier, T.; Elbert, W.; Fröhlich-Nowoisky, J.; Pöschl, U.; Pöhlker, C.; Bagheri, G.; Bodenschatz, E. Respiratory Aerosols and Droplets in the

Transmission of Infectious Diseases, 2021. arXiv:2103.01188. https://arxiv.org/abs/2103.01188.
(22) Jantunen, J.; Saarinen, K. Pollen Transport by Clothes. *Aerobiologia* **2011**, *27*, 339−343.
(23) Møller, S. A.; Rasmussen, P. U.; Frederiksen, M. W.; Madsen, A. M. Work Clothes as a Vector for Microorganisms: Accumulation, Transport, and Resuspension of Microorganisms as Demonstrated for Waste Collection Workers. *Environ. Int.* **2022**, *161*, No. 107112.
(24) Adams, R. I.; Bhangar, S.; Pasut, W.; Arens, E. A.; Taylor, J. W.; Lindow, S. E.; Nazaroff, W. W.; Bruns, T. D. Chamber Bioaerosol Study: Outdoor Air and Human Occupants as Sources of Indoor Airborne Microbes. *PLoS One* **2015**, *10*, No. e0128022.
(25) Kalweit, A.; Herrick, R. F.; Flynn, M. A.; Spengler, J. D.; Berko, J. K., Jr.; Levy, J. I.; Ceballos, D. M. Eliminating Take-Home Exposures: Recognizing the Role of Occupational Health and Safety in Broader Community Health. *Ann. Work Exposure Health* **2020**, *64*, 236−249.
(26) Deziel, N. C.; Friesen, M. C.; Hoppin, J. A.; Hines, C. J.; Thomas, K.; Freeman, L. E. B. A Review of Nonoccupational Pathways for Pesticide Exposure in Women Living in Agricultural Areas. *Environ. Health Perspect.* **2015**, *123*, 515−524.
(27) Licina, D.; Morrison, G. C.; Beko, G.; Weschler, C. J.; Nazaroff, W. W. Clothing-Mediated Exposures to Chemicals and Particles. *Environ. Sci. Technol.* **2019**, *53*, 5559−5575.
(28) Kvasnicka, J.; Cohen Hubal, E.; Ladan, J.; Zhang, X.; Diamond, M. L. Transient Multimedia Model for Investigating the Influence of Indoor Human Activities on Exposure to SVOCs. *Environ. Sci. Technol.* **2020**, *54*, 10772−10782.
(29) Licina, D.; Melikov, A.; Sekhar, C.; Tham, K. W. Transport of Gaseous Pollutants by Convective Boundary Layer around a Human Body. *Sci. Technol. Built Environ.* **2015**, *21*, 1175−1186.
(30) Licina, D.; Tian, Y.; Nazaroff, W. W. Inhalation Intake Fraction of Particulate Matter from Localized Indoor Emissions. *Build. Environ.* **2017**, *123*, 14−22.
(31) Rodes, C. E.; Kamens, R. M.; Wiener, R. W. The Significance and Characteristics of the Personal Activity Cloud on Exposure Assessment Measurements for Indoor Contaminants. *Indoor Air* **1991**, *1*, 123−145.
(32) Rim, D.; Novoselac, A. Transport of Particulate and Gaseous Pollutants in the Vicinity of a Human Body. *Build. Environ.* **2009**, *44*, 1840−1849.
(33) Al Assaad, D.; Yang, S.; Licina, D. Particle Release and Transport from Human Skin and Clothing: A CFD Modeling Methodology. *Indoor Air* **2021**, *31*, 1377−1390.
(34) Donovan, E. P.; Donovan, B. L.; McKinley, M. A.; Cowan, D. M.; Paustenbach, D. J. Evaluation of Take Home (Para-Occupational) Exposure to Asbestos and Disease: A Review of the Literature. *Crit. Rev. Toxicol.* **2012**, *42*, 703−731.
(35) Mazaheri, M.; Clifford, S.; Yeganeh, B.; Viana, M.; Rizza, V.; Flament, R.; Buonanno, G.; Morawska, L. Investigations into Factors Affecting Personal Exposure to Particles in Urban Microenvironments Using Low-Cost Sensors. *Environ. Int.* **2018**, *120*, 496−504.
(36) Koehler, K.; Good, N.; Wilson, A.; Mölter, A.; Moore, B. F.; Carpenter, T.; Peel, J. L.; Volckens, J. The Fort Collins Commuter Study: Variability in Personal Exposure to Air Pollutants by Microenvironment. *Indoor Air* **2019**, *29*, 231−241.
(37) Liu, Y.; Ning, Z.; Chen, Y.; Guo, M.; Liu, Y.; Gali, N. K.; Sun, L.; Duan, Y.; Cai, J.; Westerdahl, D.; et al. Aerodynamic Analysis of SARS-CoV-2 in Two Wuhan Hospitals. *Nature* **2020**, *582*, 557−560.
(38) Asadi, S.; Tupas, M. J.; Barre, R. S.; Wexler, A. S.; Bouvier, N. M.; Ristenpart, W. D. Non-Respiratory Particles Emitted by Guinea Pigs in Airborne Disease Transmission Experiments. *Sci. Rep.* **2021**, *11*, No. 17490.
(39) Kutter, J. S.; de Meulder, D.; Bestebroer, T. M.; Lexmond, P.; Mulders, A.; Richard, M.; Fouchier, R. A.; Herfst, S. SARS-CoV and SARS-CoV-2 Are Transmitted through the Air between Ferrets over More than One Meter Distance. *Nat. Commun.* **2021**, *12*, No. 1653.
(40) Asadi, S.; ben Hnia, N. G.; Barre, R. S.; Wexler, A. S.; Ristenpart, W. D.; Bouvier, N. M. Influenza A Virus Is Transmissible via Aerosolized Fomites. *Nat. Commun.* **2020**, *11*, No. 4062.
(41) Nazaroff, W. W. Indoor Aerosol Science Aspects of SARS-CoV-2 Transmission. *Indoor Air* **2021**, *32*, No. e12970.
(42) Nicas, M. Estimating Exposure Intensity in an Imperfectly Mixed Room. *Am. Ind. Hyg. Assoc. J.* **1996**, *57*, 542−550.
(43) Furtaw, E. J., Jr.; Pandian, M. D.; Nelson, D. R.; Behar, J. V. Modeling Indoor Air Concentrations near Emission Sources in Imperfectly Mixed Rooms. *J. Air Waste Manage. Assoc.* **1996**, *46*, 861−868.
(44) Arnold, S. F.; Shao, Y.; Ramachandran, G. Evaluating Well-Mixed Room and near-Field−Far-Field Model Performance under Highly Controlled Conditions. *J. Occup. Environ. Hyg.* **2017**, *14*, 427−437.
(45) Arnold, S. F.; Shao, Y.; Ramachandran, G. Evaluation of the Well Mixed Room and Near-Field Far-Field Models in Occupational Settings. *J. Occup. Environ. Hyg.* **2017**, *14*, 694−702.
(46) Buonanno, G.; Robotto, A.; Brizio, E.; Morawska, L.; Civra, A.; Corino, F.; Lembo, D.; Ficco, G.; Stabile, L. Link between SARS-CoV-2 Emissions and Airborne Concentrations: Closing the Gap in Understanding. *J. Hazard. Mater.* **2022**, *428*, No. 128279.
(47) Mikszewski, A.; Stabile, L.; Buonanno, G.; Morawska, L. Increased Close Proximity Airborne Transmission of the SARS-CoV-2 Delta Variant. *Sci. Total Environ.* **2021**, *816*, No. 151499.
(48) Cortellessa, G.; Stabile, L.; Arpino, F.; Faleiros, D. E.; Van Den Bos, W.; Morawska, L.; Buonanno, G. Close Proximity Risk Assessment for SARS-CoV-2 Infection. *Sci. Total Environ.* **2021**, *794*, No. 148749.
(49) Kumar, P.; Omidvarborna, H.; Tiwari, A.; Morawska, L. The Nexus between In-Car Aerosol Concentrations, Ventilation and the Risk of Respiratory Infection. *Environ. Int.* **2021**, *157*, No. 106814.
(50) Mathai, V.; Das, A.; Bailey, J. A.; Breuer, K. Airflows inside Passenger Cars and Implications for Airborne Disease Transmission. *Sci. Adv.* **2021**, *7*, No. eabe0166.
(51) Raiteux, J.; Eschlimann, M.; Marangon, A.; Rogée, S.; Dadvisard, M.; Taysse, L.; Larigauderie, G. Inactivation of SARS-CoV-2 by Simulated Sunlight on Contaminated Surfaces. *Microbiol. Spectrum* **2021**, *9*, No. e00333-21.
(52) Dabisch, P.; Schuit, M.; Herzog, A.; Beck, K.; Wood, S.; Krause, M.; Miller, D.; Weaver, W.; Freeburger, D.; Hooper, I.; et al. The Influence of Temperature, Humidity, and Simulated Sunlight on the Infectivity of SARS-CoV-2 in Aerosols. *Aerosol Sci. Technol.* **2021**, *55*, 142−153.
(53) Kasloff, S. B.; Leung, A.; Strong, J. E.; Funk, D.; Cutts, T. Stability of SARS-CoV-2 on Critical Personal Protective Equipment. *Sci. Rep.* **2021**, *11*, No. 984.
(54) Riddell, S.; Goldie, S.; Hill, A.; Eagles, D.; Drew, T. W. The Effect of Temperature on Persistence of SARS-CoV-2 on Common Surfaces. *Virol. J.* **2020**, *17*, No. 145.
(55) Owen, L.; Shivkumar, M.; Laird, K. The Stability of Model Human Coronaviruses on Textiles in the Environment and during Health Care Laundering. *mSphere* **2021**, *6*, No. e00316-21.
(56) Wang, C. C.; Prather, K. A.; Sznitman, J.; Jimenez, J. L.; Lakdawala, S. S.; Tufekci, Z.; Marr, L. C. Airborne Transmission of Respiratory Viruses. *Science* **2021**, *373*, No. eabd9149.
(57) Morawska, L.; Johnson, G. R.; Ristovski, Z. D.; Hargreaves, M.; Mengersen, K.; Corbett, S.; Chao, C. Y. H.; Li, Y.; Katoshevski, D. Size Distribution and Sites of Origin of Droplets Expelled from the Human Respiratory Tract during Expiratory Activities. *J. Aerosol Sci.* **2009**, *40*, 256−269.
(58) Milton, D. K. A Rosetta Stone for Understanding Infectious Drops and Aerosols. *Pediatr. Infect. J.* **2020**, *9*, 413−415.
(59) Volkwein, J. C.; Maynard, A. D.; Harper, M. *Workplace Aerosol Measurement*; The National Institute for Occupational Safety and Health (NIOSH), 2011; pp 571−590.
(60) Brandon, N.; Price, P. S. Calibrating an Agent-Based Model of Longitudinal Human Activity Patterns Using the Consolidated

Human Activity Database. *J. Exposure Sci. Environ. Epidemiol.* **2020**, *30*, 194−204.
(61) Brandon, N.; Dionisio, K. L.; Isaacs, K.; Tornero-Velez, R.; Kapraun, D.; Setzer, R. W.; Price, P. S. Simulating Exposure-Related Behaviors Using Agent-Based Models Embedded with Needs-Based Artificial Intelligence. *J. Exposure Sci. Environ. Epidemiol.* **2020**, *30*, 184−193.
(62) Hamby, D. M. A Review of Techniques for Parameter Sensitivity Analysis of Environmental Models. *Environ. Monit. Assess.* **1994**, *32*, 135−154.
(63) Parhizkar, H.; Dietz, L.; Olsen-Martinez, A.; Horve, P. F.; Barnatan, L.; Northcutt, D.; Van Den Wymelenberg, K. G. Quantifying Environmental Mitigation of Aerosol Viral Load in a Controlled Chamber with Participants Diagnosed with COVID-19. *Clin. Infect. Dis.* **2022**, *40*, No. ciac006.
(64) Coleman, K. K.; Tay, D. J. W.; Tan, K. S.; Ong, S. W. X.; Koh, M. H.; Chin, Y. Q.; Nasir, H.; Mak, T. M.; Chu, J. J. H.; Milton, D. K.; et al. Viral Load of SARS-CoV-2 in Respiratory Aerosols Emitted by COVID-19 Patients While Breathing, Talking, and Singing. *Clin. Infect. Dis.* **2021**, *582*, No. ciac006.
(65) Adenaiye, O. O.; Lai, J.; de Mesquita, P. J. B.; Hong, F. H.; Youssefi, S.; German, J. R.; Tai, S.-H. S.; Albert, B. J.; Schanz, M.; Weston, S.; et al. Infectious SARS-CoV-2 in Exhaled Aerosols and Efficacy of Masks During Early Mild Infection. *Clin. Infect. Dis.* **2021**, *71*, No. ciab797.
(66) Pan, M.; Lednicky, J. A.; Wu, C.-Y. Collection, Particle Sizing and Detection of Airborne Viruses. *J. Appl. Microbiol.* **2019**, *127*, 1596−1611.
(67) Schijven, J.; Vermeulen, L. C.; Swart, A.; Meijer, A.; Duizer, E.; de Roda Husman, A. M. Quantitative Microbial Risk Assessment for Airborne Transmission of SARS-CoV-2 via Breathing, Speaking, Singing, Coughing, and Sneezing. *Environ. Health Perspect.* **2021**, *129*, No. 47002.
(68) Port, J. R.; Yinda, C. K.; Owusu, I. O.; Holbrook, M.; Fischer, R.; Bushmaker, T.; Avanzato, V. A.; Schulz, J. E.; Martens, C.; van Doremalen, N.; et al. SARS-CoV-2 Disease Severity and Transmission Efficiency Is Increased for Airborne Compared to Fomite Exposure in Syrian Hamsters. *Nat. Commun.* **2021**, *12*, No. 4985.
(69) Gong, L.; Xu, B.; Zhu, Y. Ultrafine Particles Deposition inside Passenger Vehicles. *Aerosol Sci. Technol.* **2009**, *43*, 544−553.
(70) Ribaric, N. L.; Vincent, C.; Jonitz, G.; Hellinger, A.; Ribaric, G. Hidden Hazards of SARS-CoV-2 Transmission in Hospitals: A Systematic Review. *Indoor Air* **2021**, *32*, No. e12968.
(71) Asadi, S.; Cappa, C. D.; Barreda, S.; Wexler, A. S.; Bouvier, N. M.; Ristenpart, W. D. Efficacy of Masks and Face Coverings in Controlling Outward Aerosol Particle Emission from Expiratory Activities. *Sci. Rep.* **2020**, *10*, No. 15665.
(72) Chen, W.; Zhang, N.; Wei, J.; Yen, H.-L.; Li, Y. Short-Range Airborne Route Dominates Exposure of Respiratory Infection during Close Contact. *Build. Environ.* **2020**, *176*, No. 106859.
(73) Balachandar, S.; Zaleski, S.; Soldati, A.; Ahmadi, G.; Bourouiba, L. Host-to-Host Airborne Transmission as a Multiphase Flow Problem for Science-Based Social Distance Guidelines. *Int. J. Multiphase Flow* **2020**, *132*, No. 103439.
(74) Fennelly, K. P. Particle Sizes of Infectious Aerosols: Implications for Infection Control. *Lancet Respir. Med.* **2020**, *8*, 914−924.
(75) Casanova, L. M.; Jeon, S.; Rutala, W. A.; Weber, D. J.; Sobsey, M. D. Effects of Air Temperature and Relative Humidity on Coronavirus Survival on Surfaces. *Appl. Environ. Microbiol.* **2010**, *76*, 2712−2717.
(76) Leung, W. T.; Fu, S. C.; Sze To, G. N.; Chao, C. Y. H. Comparison of the Resuspension Behavior between Liquid and Solid Aerosols. *Aerosol Sci. Technol.* **2013**, *47*, 1239−1247.
(77) Nikfar, M.; Paul, R.; Islam, K.; Razizadeh, M.; Jagota, A.; Liu, Y. Respiratory Droplet Resuspension near Surfaces: Modeling and Analysis. *J. Appl. Phys.* **2021**, *130*, No. 024702.
(78) Zhao, P.; Li, Y. Modeling and Experimental Validation of Microbial Transfer via Surface Touch. *Environ. Sci. Technol.* **2021**, *55*, 4148−4161.
(79) Anderson, C. E.; Boehm, A. B. Transfer Rate of Enveloped and Non-Enveloped Viruses between Fingerpads and Surfaces. *Appl. Environ. Microbiol.* **2021**, *87*, No. e0121521.
(80) Milton, D. K. What Was the Primary Mode of Smallpox Transmission? Implications for Biodefense. *Front. Cell. Infect. Microbiol.* **2012**, *2*, No. 150.

https://doi.org/10.1021/acs.est.1c08342
Environ. Sci. Technol. 2022, 56, 5641−5652